European Conference on Optical Communication (ECOC) 2022 © Optica Publishing Group 2022

Demonstration of 6.4-Tbit/s THz-Wave Signal Transmission over 20-km Wired and 54-m Wireless Distance

Junjie Ding(1), Weiping Li(1), Long Zhang(1), Yanyi Wang(1), Jiaxuan Liu(1), Kaihui Wang(1), Li Zhao(1), Wen Zhou(1), Jiao Zhang(2), Min Zhu(2), Jianguo Yu(3), Feng Zhao(4), and Jianjun Yu(1,2)

(1) Fudan University, Shanghai, China, 200433, * jianjun@fudan.edu.cn
(2) Purple Mountain Laboratories, Nanjing, China, 211111
(3) Beijing University of Posts and Telecommunications, Beijing, China, 100876
(4) Xi'an University of Posts and Telecommunications, Xi'an, China, 710121

Abstract *The experimental demonstration of the ultra-large-capacity THz-over-fiber transmission over 20-km wired and 54-m wireless distance in an 80-channel WDM system is successfully realized, achieving a record line rate of 6.4 Tbit/s. ©2022 The Author(s)*

Introduction

Radio-over-fiber (RoF) has been widely investigated and applied to meet the demand for large-capacity services of wireless communication [1-12]. Terahertz (THz)-over-fiber technology is an important method for the design of ultra-large-capacity and long-distance THz communication, but study in this aspect is rare [13]. In our previous work, we have proposed and experimentally demonstrated a novel scheme for vector mm-wave signal generation via one single I/Q modulator based on optical asymmetric single-sideband (ASSB) modulation [14]. In this paper, ASSB modulation scheme is applied to photonics-aided THz generation and extended to WDM structure to realize ultra-large-capacity THz-over-fiber communication.

By using ASSB modulation scheme, WDM structure and advanced DSP algorithms, we successfully realize 80-channel 20-Gbaud 16QAM THz-wave signal delivery at 325 GHz over 20-km wired and 54-m wireless distance, achieving a record line rate of 6.4 Tbit/s (5.12-Tbit/s net rate). The experimental demonstration provides an effective solution for ultra-large-capacity THz-over-fiber communication in future 6G network.

Principle and experimental setup

Fig. 1 depicts the principle and experimental setup of ultra-large-capacity WDM THz-wave signal wireless transmission system. 80 WDM optical channels are produced at the transmitter, consisting of the odd-channel group (Ch. 1, 3, 5, …, 79) and the even-channel group (Ch. 2, 4, 6, …, 80). We utilize 80 ECLs operating from 1531.51 to 1563.05 nm (full tunable in the C-band) with less than 100-kHz linewidth to generate WDM channels, half of which channels in odd-channel group correspond to H18~57 channels in ITU-T standard with 100-GHz frequency spacing, while the other half in even-channel group correspond to C18~57 channels in ITU-T standard with 100-GHz frequency spacing. Two polarization-maintaining arrayed waveguide grating (PM-AWG) are added to combine the odd channels and the even channels, respectively. In the Tx off-line DSP, the generated QAM symbols from PRBS is up-sampled and filtered via a raised-cosine (RC) filter with 0.01 roll-off factor. The baseband signal is mixed with a complex sinusoidal RF source at the positive frequency f_{s1} to generate an upper sideband (USB) signal located at carrier frequency f_{s1}. The USB signal is then added with a complex sinusoidal RF source at the negative frequency - f_{s2}. Here, we set f_{s1} as 16 GHz and set f_{s2} as 9 GHz. Afterwards, we send the real and imaginary parts of generated signal into a 64-GSa/s sampling rate arbitrary waveform generator (AWG) and use the same electrical signal in all channels. The output electrical signals from four independent channels (I_{odd}, Q_{odd}, I_{even} and Q_{even}) of the AWG are boosted and fed into two 30-GHz I/Q modulators in the odd-channel and even-channel groups, respectively. After adjusting the DC-bias points of the I/Q modulator, an optical ASSB signal is generated at each optical carrier frequency f_{ci} (i=1, 2, …,80), including a modulated optical USB at frequency f_{ci}+f_{s1}, an unmodulated optical lower sideband (LSB) at frequency f_{ci}-f_{s2} as well as a significantly suppressed central optical carrier at frequency f_{ci}. Subsequently, a 3-dB polarization-maintaining optical coupler (PM-OC) is utilized to combine the optical signals in odd and even channels. A PM-EDFA is added to compensate for the insertion loss and adjust the launch optical power into the 20-km SMF-28 fiber link. The launch power into the fiber link is 0 dBm per channel. To generate THz-wave signal, a wavelength selective switch (WSS) is utilized to select the modulated optical USB of each test WDM channel and an unmodulated optical LSB from the other channel as the optical LO. When a

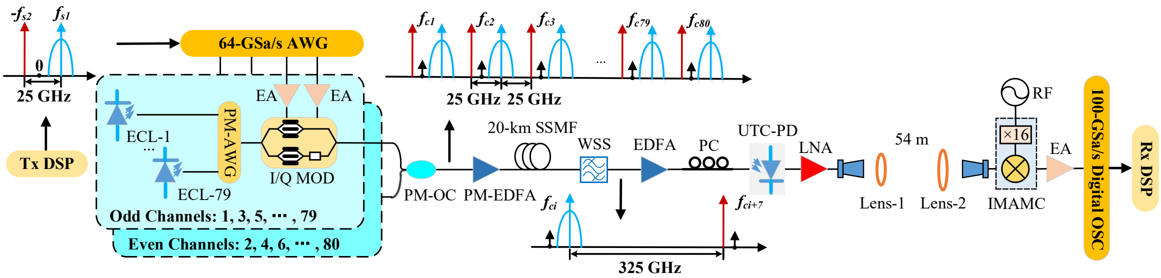

Fig. 1: Principle and experimental setup of THz-wave signal wireless transmission in an 80-channel WDM system.

modulated optical USB at optical carrier frequency f_{ci} (i≤73) is selected, an unmodulated optical LSB at optical carrier frequency f_{ci+7} should be selected as the optical LO. The frequency of the generated THz-wave signal is thus 50×7-f_{s1}-f_{s2}=325 GHz. If i>73, an unmodulated optical LSB at optical carrier frequency f_{ci-6} should be selected. In this case, the frequency of the generated THz-wave signal is also 50×6+f_{s1}+f_{s2}=325 GHz. Afterwards, an EDFA is utilized to adjust the input power into the commercial uni-travelling photodiode (UTC-PD). Besides, the polarization state of the input optical signal into the UTC-PD is controlled by a polarization controller (PC), which can maximize the strength of the generated THz-wave signal from the UTC-PD. In addition, to realize long-distance wireless delivery for the THz-wave signal, a THz-wave low-noise amplifier (LNA) with 25-dB gain is utilized.

Photos of the ultra-large-capacity THz-over-fiber communication system including transmitter, receiver as well as 54-m wireless transmission link are given in Fig. 2. In the wireless link, we utilize a pair of poly tetra fluoroethylene (PTFE) lenses (i.e., lens-1 with 10-cm diameter and 20-cm focal length, lens-2 with 30-cm diameter and 50-cm focal length) to focus the collimated THz-wave beam. At the receiver, the down-conversion of the received THz-wave signal is utilized by an integrated mixer/amplifier/multiplier chain (IMAMC), consisting of a THz-wave mixer, a 19.25-GHz RF source as well as a ×16 frequency multiplier. The output intermediate-frequency (IF) signal at 325-19.25×16=17 GHz is then boosted via an EA before captured by a 100-GSa/s sampling rate digital storge oscilloscope with 33-GHz electrical bandwidth. Finally, in the Rx-side offline DSP, the sampled data is processed by I/Q orthogonalization, 21-tap T/2-spaced CMA equalization, frequency offset estimation, hybrid principal component-based phase estimation and blind phase search (PCPE-BPS) algorithms, 171-kernel second-order Volterra nonlinear equalization (VNLE) as well as 61-tap DD-LMS equalization.

Results and discussion

After PM-EDFA, the optical spectra of 80-channel 20-GBaud signals employing 16QAM format w/o and w/ 20-km fiber transmission at 0.02-nm resolution are illustrated in Figs. 3(a) and (b), respectively. The optical spectra are non-flat due to EDFA amplification and the OSNR in short wavelength is relatively low. Figs. 3(c) and (d) gives the optical spectra of 20-GBaud 16QAM signal and optical LO at 325-GHz space before and after WSS. The selected modulated optical USB and the unmodulated optical LSB are marked in red circle.

At the wavelength of 1553.33 nm, Fig. 3 (e) gives the measured BER versus input power into UTC-PD for received 20-GBaud 16QAM and QPSK THz-wave signals in w/o and w/ 20-km

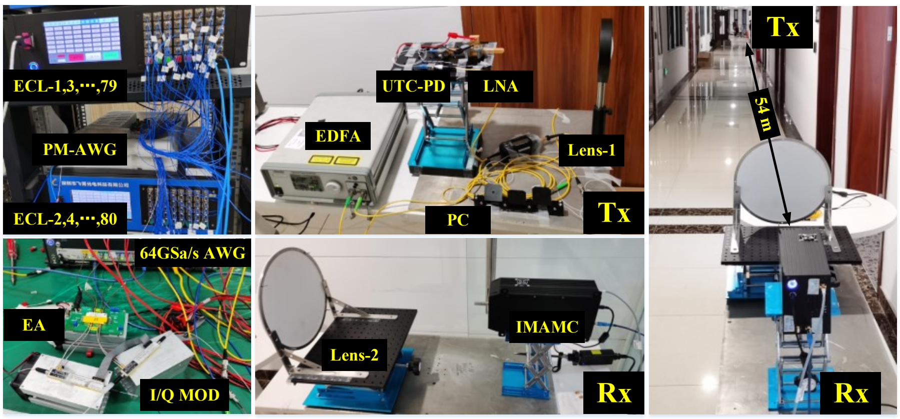

Fig. 2: Photos of experimental setup.

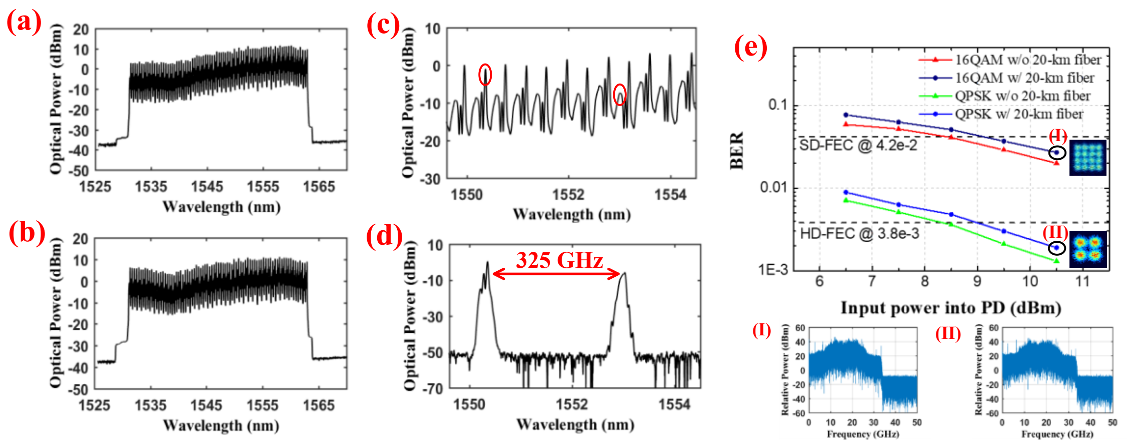

Fig. 3: Optical spectra of 80-channel 20-GBaud 16QAM signals (a) w/o and (b) w/ 20-km fiber transmission. Optical spectra of 20-GBaud 16QAM signal with 325GHz space (c) before and (d) after WSS. (e) BER versus input power into PD for 20-GBaud 16QAM and QPSK signals @ 1553.33 nm w/o and w/ 20-km fiber transmission before 54-m wireless transmission. Insets (I) and (II) are electrical spectra of the received 20-GBaud 16QAM and QPSK IF signals, respectively.

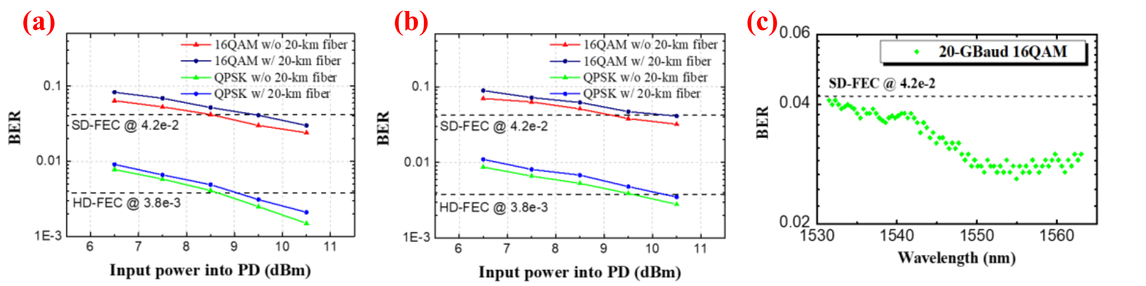

Fig. 4: BER versus input power into PD for 20-GBaud 16QAM and QPSK signals (a) @ 1563.05 nm and (b) @ 1531.51 nm w/o and w/ 20-km fiber transmission before 54-m wireless transmission. (c) BER of all 80 channels 20-Gbaud 16QAM THz-wave signals after 20-km fiber transmission and 54-m wireless transmission.

fiber transmission cases. We use the pre-FEC BER threshold of 4.2e-2 @ 25% SD-FEC and 3.8e-3 @ 7% HD-FEC [15]. It indicates that, with 20-km fiber transmission and 54-m wireless transmission, post-FEC error free can be achieved when the input power into UTC-PD reaches about 9 dBm for 20-GBaud QPSK and 16QAM THz-wave signals. Meanwhile, in w/o and w/ fiber transmission cases, the power penalty is 0.6 dB for QPSK signal at 7% HD-FEC threshold and also 0.6 dB for 16QAM signal at 25% SD-FEC threshold, which is mainly caused by the fiber loss. In addition, the electrical spectra of the received 20-GBaud 16QAM and QPSK IF signals at 10.5-dBm input power into PD are depicted in insets (I) and (II) of Fig. 3 (e). Figs. 4 (a) and (b) show the measured BER of the received 20-GBaud 16QAM and QPSK THz-wave signals w/o and w/ 20-km fiber transmission versus input power into PD at the wavelength of 1563.05 nm and 1531.51 nm, respectively. For 20-Gbaud 16QAM signal with fiber transmission in 1531.51-nm wavelength case, there is 0.8-dB power penalty at 25% SD-FEC threshold compared with the 1563.05-nm wavelength case. Besides, the power penalty is around 1.2 dB for QPSK signal with fiber transmission at 7% HD-FEC threshold. At 10.5-dBm input power into PD, we measure the BER values of 20-Gbaud 16QAM THz-wave signals in 80 channels (1531.51~1563.05 nm) after 20-km fiber transmission and 54-m wireless transmission. As shown in Fig. 4 (c), the relatively low OSNR in short wavelength results in worse BER performance and the BER values are all below the 25% SD-FEC threshold. For 20-Gbaud 16QAM signal transmission in 80-channel WDM system, the total line bit rate is 20×4×80=6.4 Tbit/s while the net bit rate is 6.4/(1+25%)=5.12 Tbit/s.

Conclusions

For the first time, we experimentally demonstrate ultra-large-capacity THz-over-fiber transmission based on WDM signal. In an 80-channel WDM system with 50-GHz spacing, the wireless transmission over 20-km wired and 54-m wireless distance utilizing 20-Gbaud 16QAM THz-wave signal reaches a record line rate of 6.4 Tbit/s.

Acknowledgements

This work is supported by National Natural Science Foundation of China (61935005, 61720106015, 61835002 and 62127802).

References

[1] C. Lim, Y. Tian, C. Ranaweera, T. A. Nirmalathas, E. Wong and K. -L. Lee, "Evolution of Radio-Over-Fiber Technology," Journal of Lightwave Technology, vol. 37, no. 6, pp. 1647-1656, 2019. DOI: 10.1109/JLT.2018.2876722.

[2] J. -i. Kani, S. Kaneko, K. Hara and T. Yoshida, "Optical Access Network Evolution for Future Super-Broadband Services and 6G Mobile Networks," European Conference on Optical Communication, 2021, Th2F.1. DOI: 10.1109/ECOC52684.2021.9606132.

[3] T. A. Nirmalathas, T. Song, S. Edirisinghe, L. Tian, C. Lim, E. Wong, K. Wang, C. Ranaweera, and K. Alameh, "Gigabit/s Optical Wireless Access and Indoor Networks," Optical Fiber Communication Conference, 2020, M2H.5. DOI: 10.1364/OFC.2020.M2H.5

[4] J. Y. Sung, K. T. Cheng, C. W. Chow, C. H. Yeh, and C.-L. Pan, "A scalable and continuous-upgradable optical wireless and wired convergent access network," Optics Express, vol. 22, pp. 12779-12784, 2014. DOI: 10.1364/OE.22.012779

[5] A. Ng'oma, "Radio-over-fiber technologies for multi-Gb/s wireless applications," Optical Fiber Communication Conference and Exposition and the National Fiber Optic Engineers Conference, 2013, OTu3E.3. DOI: 10.1364/OFC.2013.OTu3E.3

[6] T. R. Clark, J. H. Kalkavage, and E. J. Adles, "Techniques for highly linear radio-over-fiber links," Optical Fiber Communication Conference, 2017, M3E.1. DOI: 10.1364/OFC.2017.M3E.1

[7] J. Kim, M. Sung, S.I. Cho, Y. Won, B. Lim, S. Pyun, J.K. Lee, J. H. Lee, "MIMO-Supporting Radio-over-Fiber System and Its Application in mmWave-based Indoor 5G Mobile Network," Journal of Lightwave Technology, vol. 38, no. 1, pp. 101-111, 2020. DOI: 10.1109/JLT.2019.2931318

[8] C. Lim, A. Nirmalathas, "Radio-over-fiber technology: Present and Future," Journal of Lightwave Technology, vol. 39, no. 4, pp. 881-888, 2021. DOI: 10.1109/JLT.2020.3024916

[9] M. Morant, J. Prat and R. Llorente, "Radio-over-Fiber Optical Polarization-Multiplexed Networks for 3GPP Wireless Carrier-Aggregated MIMO Provision," Journal of Lightwave Technology, vol. 32, no. 20, pp. 3721-3727, 2014. DOI: 10.1109/JLT.2014.2317591

[10] R.K. Shiu, Y. Chen, P. Peng, M. Wen, S. Su, C. Hsu, G.-K. Chang, "Optical Signal Processing for W-Band Radio-Over-Fiber System with Tunable Frequency Response," Journal of Selected Topics in Quantum Electronics, vol. 27, no. 2, pp. 1-8, 2021. DOI: 10.1109/JSTQE.2020.3012598

[11] J. Y. Sung, E. Tangdiongga, T. Koonen, "A Hybrid Radio-Optical Wireless System with Efficient Sub-Centimeter Localization for Full-Coverage Indoor Services," Journal of Lightwave Technology, vol. 39, no.8, pp. 2368-2375, 2021. DOI: 10.1109/JLT.2021.3052226

[12] D. R. Kolev, M. Toyoshima, "Transmission Analysis for OFDM Signals over Hybrid RF-Optical High-Throughput Satellite," Optics Express, vol. 26, pp. 4942-4953, 2018. DOI: 10.1364/OE.26.004942

[13] T. Harter, C. Füllner, J.N. Kemal, S. Ummethala, J. L. Steinmann, M. Brosi, J. L. Hesler, E. Bründermann, A.-S. Müller, W. Freude, S. Randel and C. Koos, "Generalized Kramers–Kronig Receiver for Coherent Terahertz Communications," Nature Photonics, vol. 14, no. 10, pp. 601–606, 2020. DOI: 10.1038/s41566-020-0675-0

[14] X. Li, Y. Xu, J. Xiao, K. Wang, J. Yu, "W-Band 16QAM-Modulated SSB Photonic Vector Mm-Wave Signal Generation by One Single I/Q Modulator," Optical Fiber Communication Conference, 2017, M3E.6. DOI: 10.1364/OFC.2017.M3E.6

[15] K. Wang, L. Zhao and J. Yu, "200 Gbit/s Photonics-Aided MMW PS-OFDM Signals Transmission at W-Band Enabled by Hybrid Time-Frequency Domain Equalization," Journal of Lightwave Technology, vol. 39, no. 10, pp. 3137-3144, 2021. DOI: 10.1109/JLT.2021.3062387